Lattice Study of Dense Matter with Two Colors and Four Flavors

Simon Hands[1], Philip Kenny[1], Seyong Kim[2], and Jon-Ivar Skullerud[3]

[1] Department of Physics, College of Science, Swansea University, Singleton Park, Swansea SA2 8PP, UK
[2] Department of Physics, Sejong University, Gunja-Dong, Gwangjin-Gu, Seoul 143-747, South Korea
[3] Department of Mathematical Physics, National University of Ireland Maynooth, Maynooth, County Kildare, Ireland

Abstract. We present results from a simulation of SU(2) lattice gauge theory with $N_f = 4$ flavors of Wilson fermion and non-zero quark chemical potential μ, using the same $12^3 \times 24$ lattice, bare gauge coupling, and pion mass in cut-off units as a previous study [9] with $N_f = 2$. The string tension for $N_f = 4$ is found to be considerably smaller implying smoother gauge field configurations. Thermodynamic observables and order parameters for superfluidity and color deconfinement are studied, and comparisons drawn between the two theories. Results for quark density and pressure as functions of μ are qualitatively similar for $N_f = 2$ and $N_f = 4$; in both cases there is evidence for a phase in which baryonic matter is simultaneously degenerate and confined. Results for the stress-energy tensor, however, suggest that while $N_f = 2$ has a regime where dilute matter is non-relativistic and weakly-interacting, $N_f = 4$ matter is relativistic and strongly-interacting for all values of μ above onset.

1 Introduction

A first principles QCD-based understanding of the behaviour of dense strongly interacting matter would be of tremendous value, in part because of the theoretical interest in new phases of matter exhibiting properties such as color superconductivity and crystallisation, and also because a quantitatively accurate equation of state $\varepsilon(n_q)$, $p(n_q)$ (where ε is energy density, p pressure and n_q quark density) is a necessary input for the relativistic equations of stellar structure determining the properties of compact stellar objects. Lattice simulations, in principle the most reliable systematic non-perturbative approach to QCD, are unfortunately unavailable for dense matter, since in the presence of a quark chemical potential $\mu \neq 0$ biasing the system to have more quarks than anti-quarks, the Euclidean action is complex-valued making Monte Carlo importance sampling inoperable. Our approach to the problem is to study QC_2D, ie. Yang-Mills plus fundamental quarks with gauge group SU(2), which can be shown to have a real positive functional integral measure for an even number of quark flavors N_f. It is possible using entirely orthodox lattice QCD simulation methods to generate representative gluon field configurations and study thermodynamic properties of this model for arbitrary μ - QC_2D is thus the simplest theory in which dense matter with long-ranged inter-quark interactions can be systematically studied.

Previous work has shown that as μ is raised baryonic matter is induced to form in the ground state at an onset chemical potential $\mu_o = \frac{1}{2}m_\pi$, since the lightest baryon in the physical spectrum of QC_2D is degenerate with the pion [1,2,3]. At the same point the $U(1)_B$ baryon-number symmetry of the model is spontaneously broken by a superfluid diquark condensate [2,3,4]. Studies of the hadron spectrum confirm that in this regime there is a Goldstone excitation formed from a superposition of qq and $\bar{q}\bar{q}$ bound states [5,2,6]. There is also evidence for a change in the level ordering of π- and ρ-meson states as density increases [7,6]. Subsequent simulations probing higher densities have found evidence for degenerate quark matter and color deconfinement [8,9]. There have also been interesting studies of the glueball spectrum [10] and the presence of gauge field fluctuations with non-trivial topology [11, 12] in a dense medium.

It is, however, difficult to assess this body of work systematically, because the results have been obtained with differing lattice fermion formulations (staggered, Wilson), differing numbers of quark flavors ($N_f = 2, 4, 8$), and even differing matter representations (fundamental, adjoint). Moreover, away from the continuum limit (lattice spacing $a \to 0$) staggered lattice fermions have global invariances and symmetry breaking patterns distinct from those of the continuum theory; this has a profound effect in theories such as QC_2D having real or pseudoreal matter representations, even influencing the nature of the Sign Problem (see eg. [1]).

In this work we attempt to remedy the situation by presenting results for $N_f = 4$ obtained with the same lattice action used in previous studies with $N_f = 2$ [8,9]. It is intrinsically interesting to examine the influence of varying the matter content on the theory's ground state, especially since $N_f/N_c > 1$ in this case, although it should be immediately noted that the first two coefficients of the

renormalisation group beta-function remain negative, implying the model remains asymptotically-free and confining for $\mu, T = 0$ [1]. We will see as μ is varied that some features of the $N_f = 4$ theory are qualitatively similar to those found for $N_f = 2$, while others, particularly the behaviour of the stress-energy tensor $T_{\mu\nu}$, appear qualitatively very different. Another important difference is that for the same bare lattice gauge coupling β and pion mass $m_\pi a$ (ie. measured in cut-off units), the string tension σa^2 is much smaller for $N_f = 4$. Strictly, since the two lattice models yield distinct continuum theories, this cannot be interpreted in terms of a finer lattice; nonetheless the resulting gauge field configurations are markedly smoother for $N_f = 4$ than for $N_f = 2$, implying that the influence of at least some lattice artifacts will be diminished. In a follow-up paper [12] we will demonstrate that this makes the identification of topological excitations much easier to control, allowing their behaviour in a dense medium to be probed.

In Sec. 2 we will detail the lattice action used, and give results for the string tension measured at $\mu = 0$. The main results for quark density $n_q(\mu)$, pressure $p(\mu)$, energy density $\varepsilon(\mu)$ and trace of the stress energy tensor $T_{\mu\mu}(\mu)$ are presented in Sec. 3, as well as details of both superfluid and Polyakov line order parameters yielding information on the physical nature of the matter which forms. We will find that the main claim of [9], namely that there is a range of μ in which baryonic matter in QC$_2$D is at once degenerate (ie. having a well-defined Fermi-surface) and confined, is supported by the results of the current study. Both similarities and differences between $N_f = 4$ and $N_f = 2$ are discussed in Sec. 4.

2 Simulation Details

The lattice action used, as in previous studies in this series [8,9], employs Wilson fermions interacting with gauge fields governed by the Wilson gauge action. In units where the lattice spacing $a = 1$,

$$S = \sum_{i,j=1}^{2} \bar{\Psi}_x^i \mathcal{M}_{xy}^{ij}[U; \mu] \Psi_y^j - \frac{\beta}{N_c} \sum_{x,\nu<\lambda} \mathrm{tr} U_{\nu\lambda x}, \quad (1)$$

where $U_{\nu\lambda}$ is the oriented product of 4 SU(2)-valued link fields $U_{\nu x}$ around the sides of an elementary plaquette in the ν-λ plane, and μ is the quark chemical potential. The fields Ψ and $\bar{\Psi}$ are $8N_c$-component spinors located on the lattice sites; if we write $\Psi^i = (\varphi, \phi)^i$, then

$$\mathcal{M} = \delta^{ij} \begin{pmatrix} M[U; \mu] & \kappa j \gamma_5 \\ -\kappa j \gamma_5 & M[U; -\mu] \end{pmatrix} \quad (2)$$

with $M[U; \mu]$ the standard Wilson fermion matrix given by

$$M_{xy}[U; \mu] = \delta_{xy} - \kappa \sum_\nu \Big[(1 - \gamma_\nu) e^{\mu\delta_{\nu 0}} U_{\nu x} \delta_{y,x+\hat{\nu}}$$
$$+ (1 + \gamma_\nu) e^{-\mu\delta_{\nu 0}} U_{\nu y}^\dagger \delta_{y,x-\hat{\nu}} \Big]. \quad (3)$$

With the identifications $\psi_1 = \varphi$, $\bar{\psi}_1 = \bar{\varphi}$, $\psi_2 = (\bar{\phi}C\tau_2)^{tr}$, $\bar{\psi}_2 = (C\tau_2\phi)^{tr}$, where $C\gamma_\mu C^{-1} = -\gamma_\mu^*$ and τ_2 acts on color, the action (1) is readily seen to be equivalent to two copies of an action describing a quark isodoublet (ψ_1, ψ_2) with the usual coupling to gauge fields, with in addition a gauge invariant scalar isoscalar diquark coupling (or Majorana mass term) of the form

$$\kappa j (-\bar{\psi}_1 C\gamma_5 \tau_2 \bar{\psi}_2^{tr} + \psi_2^{tr} C\gamma_5 \tau_2 \psi_1). \quad (4)$$

A diquark source $j \neq 0$ mitigates long-wavelength fluctuations and hence critical slowing down in any superfluid phase characterised by $\langle \bar{\varphi}\gamma_5\phi \rangle \neq 0$. It explicitly breaks the global U(1)$_B$ symmetry $\varphi \mapsto e^{i\alpha}\varphi$, $\phi \mapsto e^{-i\alpha}\phi$ of (1)[2]. Alternative choices of diquark operator consistent with the Pauli Exclusion Principle are possible, but in such cases numerical simulations show no firm evidence for symmetry breaking leading to superfluidity [13]. In any case, the "physical" limit $j \to 0$ is potentially as technically and computationally challenging as the chiral limit in vacuum QCD.

It is possible to show that $\det\mathcal{M}$ is real and positive and hence that the model can be simulated using an orthodox hybrid Monte Carlo algorithm [8]. In this first study with $N_f = 4$, our strategy is to compare with results obtained for $N_f = 2$, using the same $12^3 \times 24$ lattice and bare gauge coupling $\beta = 1.9$ [9]. Since in principle the two theories have distinct physical properties, there is some arbitrariness in identifying an appropriate matching condition. In QC$_2$D the onset transition at which quark density first rises from zero signalling the transition from vacuum to baryonic matter at $T = 0$ is expected at $\mu_o = \frac{1}{2}m_\pi$ [14]. Accordingly we have chosen to match the pion mass measured *in lattice units*, ensuring that the onset happens at a similar value of μa in the two simulations. We varied κ whilst keeping fixed $\beta = 1.9$, $\mu = j = 0$, measured the pion propagator using a local source and sink, and found that $\kappa = 0.158$ yielded $m_\pi a = 0.677(14)$ in good agreement with the value $m_\pi a = 0.68(1)$ used in the $N_f = 2$ study [9].

With no further freedom, in order to set the physical scale we next measured Wilson loops with $R \times T$ with all possible spatial separations R. Fitting $W(R, T)$ to the form $Ae^{-V(R)T}$ for $aT_{\min} \geq 5$ (see Fig. 1), we use the Cornell potential

$$V(R) = C + \frac{b}{R} + \sigma R \quad (5)$$

---

[1] Note that $N_f = 4$ lies below the perturbative prediction $N_f^{BZ} \geq \frac{272}{49}$ for the existence of a conformal fixed point.

[2] In the limit $j = \mu = 0$ the full global symmetry group of the action (1) is Sp(8).
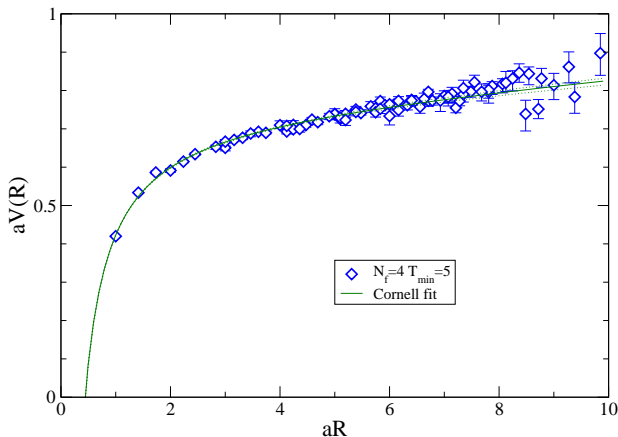
Fig. 1. The static quark potential from fits to Wilson loops with $aT \geq 5$, together with a fit to the Cornall potential (5).

to extract the string tension σ. We find $\sqrt{\sigma}a = 0.1096(64)$, yielding a lattice spacing $a = 0.052(3)$fm assuming a physical string tension $(440 \text{ MeV})^2$, about a factor of three smaller than the value $a = 0.186(8)$fm found for $N_f = 2$ [9]. Some insight may be gained by integration of the renormalisation group beta-function $\beta(g) = -a\partial g/\partial a$:

$$a = C \left(\frac{g^2}{16\pi^2 b_0 + b_1 g^2} \right)^{-\frac{b_1}{2b_0^2}} \exp \left(-\frac{8\pi^2}{b_0 g^2} \right); \quad (6)$$

with the two-loop coefficients given by

$$b_0 = \frac{11}{3}N_c - \frac{2}{3}N_f; \quad b_1 = \frac{34}{3}N_c^2 - \frac{10}{3}N_c N_f - \left(\frac{N_c^2 - 1}{N_c} \right) N_f. \quad (7)$$

Fig. 2 plots the solution (6) for $N_c = 2, 3$ and $N_f = 2, 4$.
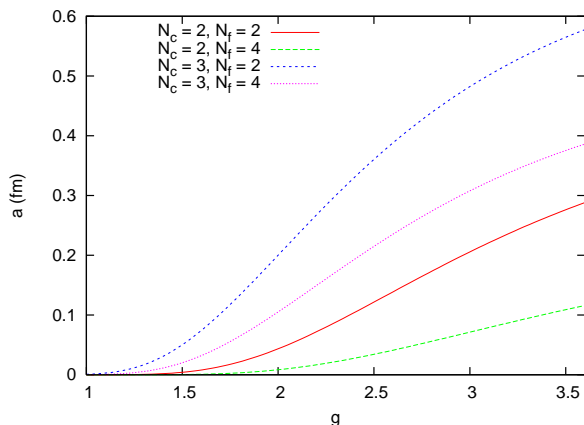
Fig. 2. *Plot of the RG equation solution (6) for $N_c = 2, 3$ and $N_f = 2, 4$.*

Whilst it is difficult to directly match the bare lattice coupling $\sqrt{2N_c/\beta}$ to the Yang-Mills coupling g plotted along the horizontal axis, it can be seen that with two colors at the "boosted" value $g \approx 2.9$, the effect of doubling the number of flavors has the same dramatic effect of reducing

a by a factor of three; in fact the constant C in (6) can be chosen so that the vertical scale of Fig. 2 matches our estimates for a made using the string tension σ. For $N_c = 3$ with the same coupling, by contrast, changing N_f from 2 to 4 reduces a by just 35%. The small lattice spacing at $N_f = 4$ is therefore not so surprising, and underlines that changing the flavor content in QC$_2$D is not as innocent as might naively be thought. It also challenges our identification of a physical scale using the string tension (particularly since we don't have the Particle Data Group to help in QC$_2$D). Taking $\sqrt{\sigma} = 440$MeV yields $m_\pi \simeq 2.6$GeV and the temperature of the lattice $T \simeq 160$MeV, which on the face of it makes comparison with the results of [9] difficult.

Without data at different values of a enabling a continuum extrapolation, the best we can achieve in this inital study of flavor-rich dense matter is therefore a comparison of $N_f = 2, 4$ in pion-mass units, since the two simulations have matched values of $L_s m_\pi$, $L_t m_\pi$, and in the $T \to 0$, $j \to 0$ limits should manifest the onset of baryonic matter at the same value of μ_o/m_π (recall also that from both theoretical [14] and simulational [1] standpoints, the best way to present data obtained for $\mu \gtrsim \mu_o$ with different quark masses uses units of μ/m_π). As a result, the figures plotted in Sec. 3 all start to exhibit non-trivial behaviour at the same point along the μ-axis.

We should bear in mind that at $N_f = 4$ the gauge field configurations are likely to be significantly smoother and hence lattice artifacts smaller. A potential worry is that the $N_f = 4$ simulations are much more susceptible to finite-volume artifacts and thermal effects as a result of the much smaller values of $L_s\sqrt{\sigma}$ and $L_t\sqrt{\sigma}$.

3 Numerical Results at $\mu \neq 0$

The action (1) was used to generate between 300 - 500 HMC trajectories of mean length 0.5 for chemical potentials $\mu a \in [0.25, 1.2]$, with diquark source $ja = 0.04$ throughout. The molecular dynamics timestep needed to maintain 75% acceptance ranged from $dt = 0.004$ at $\mu a = 0.25$ to $dt = 0.002$ at $\mu a = 1.0$. Fig. 3 shows results for the primary thermodynamic observable, the quark density $n_q(\mu) \equiv -\partial \ln \mathcal{Z}/\partial \mu$, for both $N_f = 4$ and $N_f = 2$ [9]. What is actually plotted is the dimensionless ratio n_q/n_{SB}^{latt}, where n_{SB}^{latt} is the quark density evaluated on the same $12^3 \times 24$ lattice with free massless quarks, ie. with $\beta = \infty, \kappa = \frac{1}{8}$. The purpose of this is to compensate for both finite-volume effects and lattice artifacts [8]. Note that for $T = 0$ in the thermodynamic and continuum limits,

$$n_{SB}^{\text{cont}}(\mu) = \frac{N_f N_c}{3\pi^2} \mu^3, \quad (8)$$

characteristic of a degenerate system with $E_F = k_F = \mu$.

The most striking feature of Fig. 3 is the qualitative similarity of the $N_f = 2$ and $N_f = 4$ data when expressed in cut-off units. In both cases n_q/n_{SB}^{latt} rises sharply from near the theoretical onset at $\mu_o \approx \frac{1}{2}m_\pi = 0.34a^{-1}$
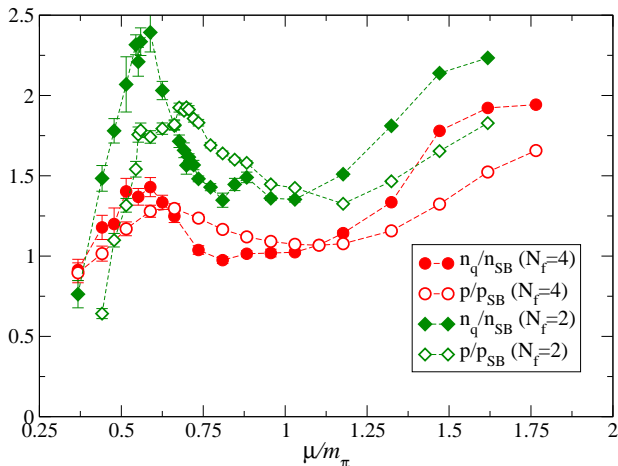
Fig. 3. n_q/n_{SB}^{latt} and p/p_{SB}^{latt} vs. μ/m_π for $N_f = 2, 4$.

to a maximum at $\mu/m_\pi \approx 0.6$ before falling. This non-monotonic behaviour is predicted in chiral perturbation theory (χPT) [14,8], which treats the matter forming at onset as a Bose-Einstein condensate of deeply bound scalar isoscalar diquark pairs. In fact beyond the maximum, χPT predicts the ratio to be monotonically falling, proportional to μ^{-2} as $\mu \to \infty$. By contrast, at a value $\mu = \mu_Q \approx 0.75m_\pi$ the measured ratio levels off; moreover, for $N_f = 4$ the ratio is close to unity over the range $0.75 \lesssim \mu/m_\pi \lesssim 1.0$. Finally, for $\mu > \mu_D \approx 1.0m_\pi$ the ratio starts to rise again.

In [9] the behaviour for $\mu \in (\mu_Q, \mu_D)$ was interpreted as a regime where the fermionic nature of the quarks has become manifest, resulting in the formation of a Fermi surface only weakly perturbed by diquark condensation (see below). In other words, the threshold value μ_Q corresponds to a BEC/BCS crossover. The new data at $N_f = 4$ strengthens this interpretation, since the ratio is now so close to one; indeed n_q/n_{SB}^{latt} seems to approach unity from above as $a \to 0$. Since, however, care must be exercised when extrapolating to the continuum limit using data from distinct theories, and also because the necessary $j \to 0$ extrapolation is still to be done, we cannot say at this stage whether any physical significance should be attached to the differing heights of the peaks at $\mu/m_\pi = 0.6$. The flatness of the $N_f = 4$ data in this regime does however increase our confidence in the rather *ad hoc* procedure for mitigating lattice artifacts by taking the ratio of interacting to free theories, which can only strictly be justified if a continuum limit is taken.

Fig. 3 also plots the pressure p for both theories, obtained by integrating the Maxwell relation $n_q = \partial p/\partial \mu$. For the lattice data we have implemented this via the formula [8]

$$\frac{p}{p_{SB}^{\text{latt}}}(\mu) = \frac{\int_{\mu_o}^{\mu} \frac{n_{SB}^{\text{cont}}}{n_{SB}^{\text{latt}}}(\mu')n_q(\mu')d\mu'}{\int_{\mu_o}^{\mu} n_{SB}^{\text{cont}}(\mu')d\mu'}, \qquad (9)$$

with the integrals estimated by an extended trapezoidal rule. Since the data for p derive from those for n_q, most of the qualitative comments made above apply here also.

We note that the $N_f = 4$ curve is smoother, and that once again the ratio p/p_{SB} is close to unity in the range $\mu \in (\mu_Q, \mu_D)$.
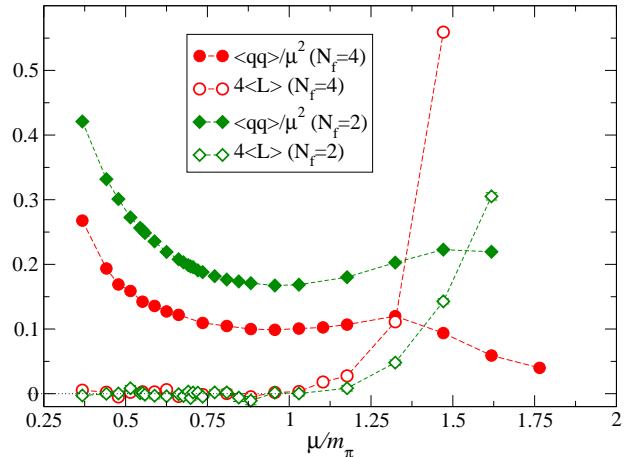

Fig. 4. $\langle qq \rangle/\mu^2$ and rescaled Polyakov line vs. μ/m_π for $N_f = 2, 4$.

In order to characterise the properties of the different regions better, in Fig. 4 we plot two further important observables, the superfluid order parameter $\langle qq \rangle \equiv \frac{\kappa}{2}\langle\bar{\varphi}\gamma_5\phi - \bar{\phi}\gamma_5\varphi\rangle$, and the Polyakov line $\langle L \rangle = \frac{1}{N_c}\text{tr}\langle\prod_{t=1}^{L_t} U_{0;\boldsymbol{x},t}\rangle$. Once again, the results for $N_f = 4$ are qualitatively very similar to those found for $N_f = 2$. Note that $\langle qq \rangle$ is strictly only an order parameter in the limit $j \to 0$; we choose to plot the ratio $\langle qq \rangle/\mu^2$ since for a degenerate system in which superfluidity arises as a result of BCS condensation the order parameter is expected to scale as the area of the Fermi surface via $\langle qq \rangle \propto \Delta_{BCS}\mu^2$, where Δ_{BCS} is the superfluid gap. Fig. 4 confirms that this is indeed the case for $\mu \in (\mu_Q, \mu_D)$; the data for $N_f = 4$ being flatter than those for $N_f = 2$, although both manifest a shallow minimum at $\mu/m_\pi \approx 0.95$. This suggests the inequality

$$\Delta_{BCS}^{N_f=4}a < \Delta_{BCS}^{N_f=2}a. \qquad (10)$$

Whilst this may signal a physical difference between the two theories, the influence of lattice artifacts, or indeed the opening up of other more favoured condensation channels in the flavor-rich case, cannot yet be eliminated.

Fig. 4 also shows a sharp transition between $\langle L \rangle \approx 0$ and $\langle L \rangle > 0$ at $\mu_D \approx 1.0m_\pi$. This transition approximately coincides with the upturn in n_q/n_{SB}^{latt} observed in Fig. 3. Since $\langle L \rangle \sim \exp(-f_q/T)$, where f_q is the free energy of a static isolated color source, we interpret μ_D as the chemical potential at which color deconfinement takes place. It is striking that $\mu_D^{N_f=2}/m_\pi$ and $\mu_D^{N_f=4}/m_\pi$ appear to be identical; we attribute the difference in magnitude of $\langle L \rangle$ for $\mu > \mu_D$ to the smoother gauge fields for $N_f = 4$, resulting in a smaller downwards renormalisation of the Polyakov line [15].

We therefore recover for QC$_2$D with $N_f = 4$ the same intriguing result found for $N_f = 2$ [9]; namely that for low

temperatures $T \ll \mu$, $\mu_D > \mu_Q$, implying that there is a phase with the thermodynamic properties of degenerate quark matter, but in which color is confined. The current result is if anything stronger than that of [9] because $n_q(\mu)$ approaches the free quark result much more closely as a result of the smoother gauge fields. Such a phase is reminiscent of the confined, chirally-symmetric *quarkyonic* phase originally discussed in the context of large-N_c gauge theories [16]. Unfortunately our use of Wilson lattice fermions, which have no chiral symmetry away from the limit $\kappa \to \kappa_c$, precludes a discussion of whether chiral symmetry is restored for $\mu > \mu_Q$ at present.
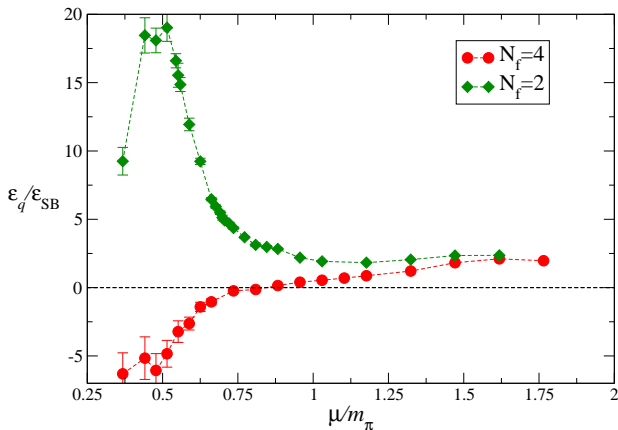

Fig. 5. $\varepsilon_q / \varepsilon_{SB}^{latt}$ *vs.* μ/m_π *for* $N_f = 2, 4$.

So far we have found a close similarity between $N_f = 2$ and $N_f = 4$. This does not carry over to the quark energy density ε_q, defined here by

$$\varepsilon_q = \kappa \sum_{i=1}^{N_f} \Big\langle \bar{\psi}_x^i (\gamma_0 - 1) e^{\mu} U_{0x} \psi_{x+\hat{0}}^i - $$
$$\bar{\psi}_x^i (\gamma_0 + 1) e^{-\mu} U_{0x-\hat{0}}^\dagger \psi_{x-\hat{0}}^i \Big\rangle. \quad (11)$$

Fig. 5 plots $\varepsilon_q / \varepsilon_{SB}^{latt}$ versus μ for $N_f = 2, 4$. Note that a vacuum contribution ε_q^0 evaluated at $\mu = 0$ must be subtracted from both interacting and free data; for $N_f = 4$ this correction $\varepsilon_q^0 a^4 = 0.3724(10)$. Even after this additive correction there is still a multiplicative renormalisation required by a μ-independent factor known as a Karsch coefficient [17]. Non-perturbative values for Karsch coefficients are still to be determined for QC$_2$D, but the shapes of the curves are in principle correct up to discretisation errors. Fig. 5 shows a big difference at low values of μ between $N_f = 2$, where $\varepsilon_q / \varepsilon_{SB}^{latt}$ has a peak considerably larger than that predicted by χPT [8,9], and $N_f = 4$, where the ratio actually starts negative and rises monotonically with μ. A negative value of ε_q is not forbidden *a priori*, but the requirement for positivity of the total energy density certainly constrains the contribution ε_g from the gluons (see below). For $\mu \gtrsim \mu_D$ $\varepsilon_q^{N_f=2}/\varepsilon_{SB}^{latt} \approx 2$ becomes approximately constant; $\varepsilon_q^{N_f=4}/\varepsilon_{SB}^{latt}$ approaches this value

from below, and for $\mu/m_\pi \gtrsim 1.5$ the two models appear to coincide up to the unknown Karsch correction.
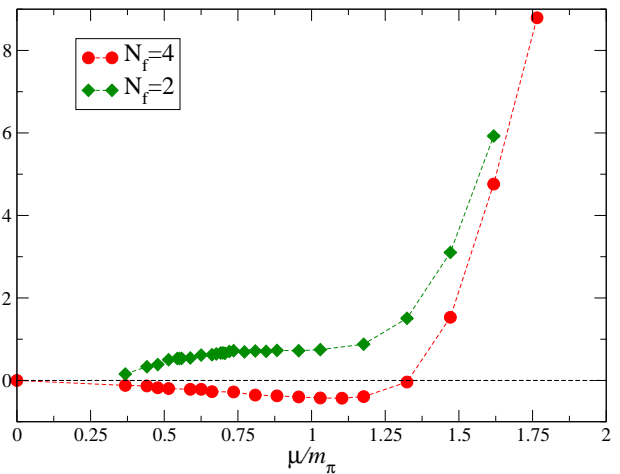
Fig. 6. *The unrenormalised quark contribution to the trace anomaly* $\kappa^{-1} Tr(\mathbf{1} - \langle \bar{\psi}\psi \rangle)$ *vs.* μ/m_π *for* $N_f = 2, 4$.

A related quantity is the quark contribution to the trace of the stress-energy tensor $(T_{\mu\mu})_q$, given by

$$(T_{\mu\mu})_q = a \frac{\partial \kappa}{\partial a} \times \frac{1}{\kappa} (4 N_f N_c - \langle \bar{\psi}\psi \rangle). \quad (12)$$

With data from only one lattice spacing, we are currently unable to estimate the beta-function; Fig. 6 plots raw values of $\kappa^{-1}\mathrm{Tr}(\mathbf{1} - \langle \bar{\psi}\psi \rangle)$ for $N_f = 2, 4$, normalised to two quark flavors for ease of comparison, and including the necessary vacuum subtraction. Qualitatively they have very different behaviour for $\mu < \mu_D$, and suggest that $(T_{\mu\mu})_q^{N_f=2}$ and $(T_{\mu\mu})_q^{N_f=4}$ differ even in sign in this regime. Note that χPT predicts $T_{\mu\mu} > 0$ for $\mu_o < \mu < \sqrt{3}\mu_o$ [8]. Since $T_{\mu\mu} = \varepsilon - 3p$ for isotropic matter, the negative sign of $(T_{\mu\mu})_q^{N_f=4}$ is consistent with the negative value of ε_q for small μ reported in the previous paragraph. Once $\mu \gtrsim \mu_D$, both models exhibit a strong upward trend, suggesting that quarks dominate $T_{\mu\mu}$ in the deconfined phase.

Finally we present results for local gluonic observables. In a non-Lorentz invariant system such as one with $\mu \neq 0$ it is helpful to define

$$\Box_s = \frac{1}{3N_c} \sum_{i<j} \langle \mathrm{tr} U_{ijx} \rangle; \quad \Box_t = \frac{1}{3N_c} \sum_x \sum_i \langle \mathrm{tr} U_{0ix} \rangle. \quad (13)$$

We then consider in Fig. 7 the difference, proportional to the gluon energy density

$$\varepsilon_g = 3Z\beta(\Box_t - \Box_s), \quad (14)$$

where Z is another as yet undetermined Karsch coefficient (assumed unity in the figure), and in Fig. 8 the average plaquette related to the gluon component of the stress-energy tensor via

$$(T_{\mu\mu})_g = -a \frac{\partial \beta}{\partial a} \times 3\beta(\Box_s + \Box_t). \quad (15)$$
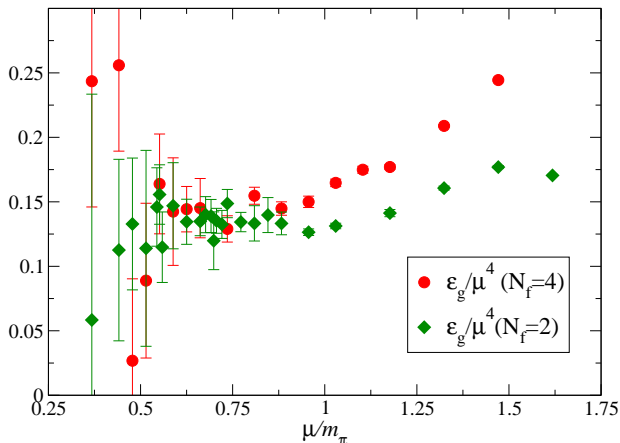
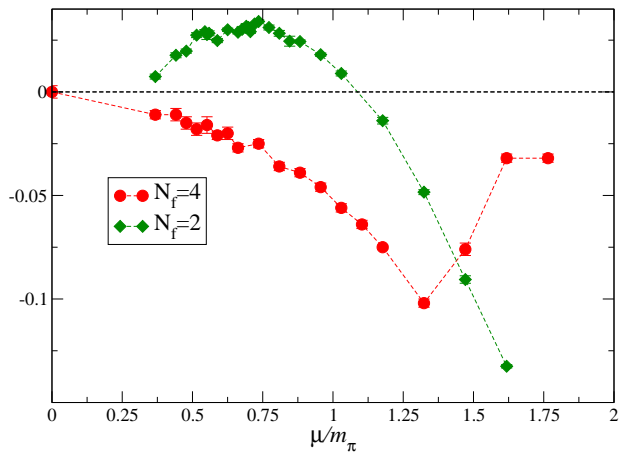**Fig. 7.** ε_g/μ^4 vs. μ/m_π for $N_f = 2, 4$.

Fig. 8. *The unrenormalised gluon contribution to the trace anomaly* $3\beta(\square_s + \square_t)$ *vs.* μ/m_π *for* $N_f = 2, 4$.

For the gluon energy density (Fig. 7) we have no analytic expectation from either free field theory or χPT. As in previous work, we plot the dimensionless quantity ε_g/μ^4; modulo the Karsch coefficient its value for $\mu \lesssim \mu_Q$ is approximately constant and similar in magnitude for $N_f = 2, 4$ (at the smallest μ the errors are hard to control), but for $\mu \gtrsim \mu_D$ the ratio increases faster for $N_f = 4$, and has essentially doubled by $\mu/m_\pi = 1.5$. For $(T_{\mu\mu})_g$ (Fig. 8) we note that again a vacuum subtraction must be applied. It is clear that there is a regime $\mu_o \lesssim \mu \lesssim \mu_D$ where $(T_{\mu\mu})_g^{N_f=2}$ is positive, before turning over to become negative at large μ; by contrast $(T_{\mu\mu})_g^{N_f=4} < 0$ throughout. It is not yet clear whether the sharp upward kink at $\mu/m_\pi = 1.3$ is physical, or merely a discretisation artifact.

The data of Figs. 6,8 taken together imply a major qualitative difference between $N_f = 2$ and $N_f = 4$: in the former case, $T_{\mu\mu} > 0$ for all μ, which in particular is consistent with the existence of a non-relativistic description with $\varepsilon \gg p$ for $\mu \gtrsim \mu_o$. For $N_f = 4$ by contrast, $T_{\mu\mu} < 0$ for $\mu < \mu_D$ (we are unable to make a firm statement at this point about the deconfined phase due to the

absence of the beta-functions), implying that the matter which forms at onset is already strongly-interacting and relativistic.

4 Discussion

In this paper we have presented the first exploratory results for flavor-rich baryonic matter with $N_f = 4$ in QC$_2$D. Since available resources have restricted us to a single lattice spacing, hopping parameter and diquark source strength, we have chosen to match the simulation to a previous study of $N_f = 2$ on the same lattice size with the same value of $m_\pi a$ [9], implying the same onset chemical potential $\mu_o a$ measured in lattice units. Accordingly the comparison between the two theories is best performed using observables measured in units of m_π. Since $\sigma^{N_f=4} a^2 < \sigma^{N_f=2} a^2$, we expect the lattice gauge fields to be much smoother in the flavor-rich case, although that renders results more susceptible to finite-volume and thermal corrections due to the corresponding reduction in $L_s\sqrt{\sigma}$, $L_t\sqrt{\sigma}$. One particular concern in the latter case is that the static potential $V(R)$ used to calibrate the lattice could actually be underestimated due to thermal screening. Another caveat which must eventually be addressed is control over the extrapolation to continuum $a \to 0$ and zero source $j \to 0$ limits, currently being addressed for $N_f = 2$ [18].

Let us cite one example of a potential issue in the current study, the total energy density ε. If we make the most optimistic assumption that the Karsch coefficients are approximately unity, and that both $j \to 0$ and $a \to 0$ extrapolations will not change the results much, then the data of Figs. 5,7 suggest that for $\mu \sim \mu_o$ with $N_f = 4$ $\varepsilon/\mu^4 = \varepsilon_q/\mu^4 + \varepsilon_g/\mu^4 \approx -0.7 + 0.13 < 0$, which is clearly unphysical.

We also note that at $\mu/m_\pi = 1.76$, the largest chemical potential studied, the ratio $n_q^{N_f=4}/n^{\text{sat}} = 0.32$, where $n^{\text{sat}} = 2N_f N_c$ is the saturation density obtained when every lattice site is maximally occupied by fermionic degrees of freedom; hence we might be concerned that in this high-density regime the results are susceptible to saturation artifacts. In this light, the superfluid condensate in Fig. 4 and gluon contribution to the stress-energy tensor in Fig. 8 are especially troubling, since both show a sharp kink at $\mu/m_\pi = 1.3$, for which we currently have no explanation.

Bearing these caveats in mind, let us review the principal results. Fig. 3 for n_q, p for $N_f = 2, 4$ expressed as fractions of the free-field results, demonstrates that both models display a qualitatively similar sequence of transitions as μ is increased. For $N_f = 4$ there is a range $0.75 < \mu/m_\pi < 1.0$ where $n_q/n_{SB}^{\text{latt}} \approx 1$, implying the existence of a well-defined Fermi surface. Further study will be needed to establish whether the difference in the height of this plateau results from the diminished impact of lattice artifacts in the $N_f = 4$ simulation, or a genuine physical difference between the two theories. Still, the enhanced flatness of the $N_f = 4$ plateau and the plausibility of the resulting physical picture increases our confidence in the

slightly *ad hoc* procedure we have used to compensate for discretisation artifacts.

Another result is the confirmation of the major finding of [9], namely that $\mu_D > \mu_Q$, or in other words, for both $N_f = 2$ and 4 there is a range of μ where degenerate quark matter remains color-confined. It will be very interesting to elucidate the nature of the deconfined phase further, since at first sight it bears little resemblance to thermal deconfinement. For instance, Fig. 7 suggests that the gluon energy density rises smoothly for $\mu \gtrsim \mu_D$, with ε_g/μ^4 increasing by at most a factor of two over its value near onset.

Finally, the most interesting and unexpected feature of the new simulation is the big difference between $N_f = 2, 4$ for the quark contributions to the energy density (Fig. 5) and stress-energy tensor (Fig. 6). For moderate μ both $\varepsilon_q^{N_f=4}$ and $(T_{\mu\mu})_q^{N_f=4}$ are negative; this result is self consistent and independent of the value of the relevant Karsch coefficient, though as discussed above could potentially alter as the limits $a \to 0$, $j \to 0$ are taken. The disparity between $N_f = 2$ and 4 however, and of each with the predictions of χPT [8], is striking. It suggests very different physical descriptions in the low-density regime: as $\mu \to \mu_{o+}$ the $N_f = 2$ theory appears to be a non-relativistic BEC formed of weakly-interacting tightly-bound diquark bosons, consistent with χPT [14] and yielding $T_{\mu\mu} > 0$, whereas with $N_f = 4$ the matter appears to be relativistic and strongly-interacting for all $\mu > \mu_o$.

References

1. S.J. Hands, I. Montvay, S.E. Morrison, M. Oevers, L. Scorzato and J.I. Skullerud, Eur. Phys. J. C **17** (2000) 285.
2. J.B. Kogut, D.K. Sinclair, S.J. Hands and S.E. Morrison, Phys. Rev. D **64** (2001) 094505
3. R. Aloisio, V. Azcoiti, G. Di Carlo, A. Galante and A. F. Grillo, Nucl. Phys. B **606** (2001) 322.
4. S.J. Hands, I. Montvay, L. Scorzato and J. Skullerud, Eur. Phys. J. C **22** (2001) 451.
5. S.J. Hands, J.B. Kogut, M.P. Lombardo and S.E. Morrison, Nucl. Phys. B **558** (1999) 327.
6. S. Hands, P. Sitch and J.I. Skullerud, Phys. Lett. B **662**, 405 (2008).
7. S. Muroya, A. Nakamura and C. Nonaka, Phys. Lett. B **551** (2003) 305.
8. S. Hands, S. Kim and J.I. Skullerud, Eur. Phys. J. C **48** (2006) 193.
9. S. Hands, S. Kim and J.I. Skullerud, Phys. Rev. D **81** (2010) 091502(R).
10. M.P. Lombardo, M.L. Paciello, S. Petrarca and B. Taglienti, Eur. Phys. J. C **58**, 69 (2008).
11. B. Alles, M. D'Elia and M.P. Lombardo, Nucl. Phys. B **752**, 124 (2006).
12. S.J. Hands and P. Kenny, [arXiv:1104.0522 [hep-lat]]
13. P. Kenny, Ph.D. thesis, Swansea University (2010).
14. J.B. Kogut, M.A. Stephanov, D. Toublan, J.J.M. Verbaarschot and A. Zhitnitsky, Nucl. Phys. B **582** (2000) 477.
15. S. Gupta, K. Huebner and O. Kaczmarek, Phys. Rev. D **77** (2008) 034503.
16. L. McLerran and R.D. Pisarski, Nucl. Phys. A **796** (2007) 83.
17. F. Karsch and I.O. Stamatescu, Phys. Lett. B **227**, 153 (1989).
18. S. Hands and J.I. Skullerud, in preparation.